Structure of Wave Functions of Pseudointegrable Billiards

E. Bogomolny and C. Schmit

*Laboratoire de Physique Théorique et Modèles Statistiques**, *Université de Paris-Sud, Bâtiment 100, 91405 Orsay Cedex, France*

(Received 12 February 2004; published 16 June 2004)

Wave functions of pseudointegrable plane polygonal billiards are investigated. It is demonstrated that they have clear structures (superscars) related with families of classical periodic orbits which do not disappear at large energy.

DOI: 10.1103/PhysRevLett.92.244102 PACS numbers: 05.45.Mt, 03.65.Sq, 42.25.Fx

A central problem of quantum chaos is an adequate description of different types of quantum systems which do not permit an exact solution. For example, it is well accepted that eigenenergies of chaotic systems are distributed as eigenvalues of random matrix ensembles [1], and their eigenfunctions are described by Gaussian random functions [2]. But much less is known when a model is neither chaotic nor integrable.

Particular intriguing examples are plane polygonal billiards whose classical mechanics is surprisingly rich. When all their angles are rational with π these models are called pseudointegrable (PI) because their classical trajectories cover two-dimensional surfaces of genus $g > 1$ (see, e.g., [3]). It was established numerically [4] that spectral statistics of PI models in many aspects resembles statistics of the Anderson model at the metal-insulator transition [5]. In particular, the nearest-neighbor distribution displays a repulsion at small distances and an exponential decay at large separations.

The purpose of this Letter is to investigate wave functions of certain PI systems. It is found that they have a superscarring property; namely, many of them have clear structures connected with families of classical periodic orbits which, it seems, do not disappear at large energy.

The scar phenomenon in chaotic systems is not new. The existence of structures near unstable periodic orbits in chaotic wave functions was established in [6] and later many works were done to clarify the subject (see, e.g., [7] and references therein). PI systems differ in many aspects from chaotic and integrable systems and to the authors' knowledge no conjecture about their wave functions exists in the literature.

The main difficulty with analytical treatment of PI models is the strong diffraction on billiard corners with angles $\neq \pi/n$ with integer n. When a bunch of parallel classical trajectories hits these singular corners it splits discontinuously into two different bunches whose boundaries are called optical boundaries. Quantum mechanics smooths such singularities and associates with them scattering amplitudes [8] which due to discontinuous splitting of classical trajectories have different asymptotics at large distances in different regions bounded by optical boundaries. An especially complicated case corresponds to multiple scattering when optical boundaries for different centers are close to each other. Up to now, due to the singular character of such a diffraction, it has been proved analytically only that the two-point correlation form factor for certain PI models takes at the origin a finite value different from standard statistics [9].

For PI systems classical periodic orbits form continuous families of parallel trajectories restricted by singular corners. Hence, waves traveling in such periodic orbit channels (POC) are influenced by infinite periodic arrays of singular diffractive centers. Fortunately, for the scattering on a staggered periodic array of half planes this problem has an exact solution found in [10] by the Wiener-Hopf method. In [11] this solution was analyzed in the semiclassical limit of large energy, and it was found that in the most singular case when the incidence angle (with respect to a plane formed by half-plane ends) is going to zero, all transmission and reflection coefficients tend also to zero except the "elastic" reflection coefficient (corresponding to the specular reflection from this plane) which goes to -1. It means that the fictitious scattering plane passing through singular diffraction corners plays the role of a perfect mirror with the Dirichlet boundary conditions. This mirror does not really exist, but the multiple scattering on an infinite number of parallel half planes is equivalent to the reflection on this mirror plus corrections given by complicated formulas (see [11]) and governed by the perturbation parameter

$$u = \sqrt{kl}\varphi, \tag{1}$$

where φ is the incidence angle with respect to the scattering plane, l is the distance between singular corners along the scattering plane, and $k = \sqrt{E}$ is the wave momentum. Hence, when $u \to 0$ (and $k \to \infty$) the dominant approximation to the discussed multiple scattering problem consists of treating scattering planes as true mirrors on which the total wave tends to zero.

After unfolding each periodic orbit family in PI models corresponds to an infinite POC restricted from both sides by straight lines passing through singular corners called singular diagonals (SD). When a wave with a small u moves inside such a channel, it reflects back and forth from SD as from perfect mirrors forming a propagating wave with zero boundary conditions on SD analogous to

the Borrmann effect for scattering in crystals [12]. Therefore, in each POC one can construct quasistates which we call unfolded scar states with the following properties: (i) they have a small perturbation parameter (1), (ii) they obey the Dirichlet boundary conditions on SD, and (iii) they are periodic (or antiperiodic) along POC;

$$\Psi_{m,n}^{(\mathrm{scars})}(\xi,\eta) \sim \sin\left(\frac{\pi}{l} m\xi + \delta\right)\sin\left(\frac{\pi}{w} n\eta\right)\chi(\eta). \qquad (2)$$

Here ξ and η ($0 < \eta < w$) are coordinates, respectively, along and perpendicular to POC, l is the length of POC equal to the length of primitive periodic trajectory, w is the channel width, $m, n \geq 1$ are integers, and δ is a phase related with the choice of coordinates. $\chi(x)$ in (2) is the characteristic function of POC [$\chi(x) = 1$ or 0 when x is, respectively, inside or outside POC] introduced to stress that scar states exist only inside POC. The bulk energy of such a scar state is

$$E_{m,n} = \left(\frac{\pi}{l}\right)^2 m^2 + \left(\frac{\pi}{w}\right)^2 n^2. \qquad (3)$$

Folding back the scar state (2) leads to a complicated expression $\Psi_{m,n}^{(\mathrm{scar})}(x, y)$ which can be represented in a suitable expansion basis for any system. Folded scar states (i) obey the correct boundary conditions on billiard boundaries and (ii) fulfill the equation $(\Delta + E_{m,n})\Psi_{m,n}^{(\mathrm{scar})}(x, y) = 0$ everywhere except on SD.

The above scar states exist only if the perturbation parameter (1) is small. As $\varphi \approx \pi n/wk$ the criterion of existence of a strong scar state with energy (3) is

$$1 \leq n \leq n_{\max} \quad \text{and} \quad n_{\max} \sim w\sqrt{k/l}. \qquad (4)$$

This inequality implies that any POC in PI models supports scar states with fixed n when $k \to \infty$ in marked contrast with the scarring on unstable periodic orbits where contributions from individual orbits tend to zero in semiclassical limit. To stress this difference we propose to refer to such scars as to superscars.

The total number of scar states depends on the system considered. Only for special type of PI models called Veech polygons [13] (see also [1]) analytical calculations are possible. For such systems (i) the number of POC with $l < L$ has the quadratic asymptotics

$$N(l < L) \overset{L\to\infty}{\to} CL^2/A, \qquad (5)$$

where A is the billiard area, C is a system dependant constant, and (ii) the width of POC with length l is

$$w = \gamma A/l, \qquad (6)$$

where $\gamma < 1$ is a constant taken from a finite set.

Using (4) and these formulas one concludes that (i) scar states exist only for POC whose length is restricted:

$$l \leq l_{\max} \quad \text{with} \quad l_{\max} \sim k^{1/3} \qquad (7)$$

(other channels are closed and cannot support propagating waves with $n \geq 1$) and (ii) the averaged density of scar states $\bar{\rho}_s$ is of the same order as the mean total density of states $\bar{\rho}$:

$$\bar{\rho}_s = \sum_{\mathrm{scars}} \delta(E - E_{m,n}) \sim \sum_{l<l_{\max}} \frac{l}{k} n_{\max} \sim \bar{\rho}. \qquad (8)$$

These results show that for PI models where (5) and (6) hold scar states are a good zero-order approximation to wave functions. As an illustration consider, e.g., the right triangle with angle $\pi/8$. Its simplest POC corresponds to orbits perpendicular to the shortest side of the triangle. After unfolding it has a rectangular shape as indicated in Fig. 1(a). The folded scar state for this POC is shown schematically in Fig. 1(b). Dashed lines in this figure indicate maxima of the scar state. They have a complicated form except at the right corner of the triangle where they form horizontal lines.

In Figs. 1(c)–1(e) three true eigenfunctions of this triangular billiard (with area 4π) are presented. The eigenfunctions were chosen because their energies are close to the scar energy (3) calculated with $l = a$ and $w = b$, where a and $b = a\tan\pi/8$ are sides of the triangle. The characteristic horizontal lines corresponding to the scar picture [as in Fig. 1(b)] are clearly seen in all these eigenfunctions. These pictures are just a few examples (among many others) of clear scar eigenfunctions observed in triangular billiards. Complicated folding of POCs in such models makes it difficult to visualize scar states associated with longer trajectories. This goal can more easily be achieved in another PI model, called barrier billiard (BB), which in the simplest case consists of a rectangular billiard with the Dirichlet boundary conditions on all sides except the half of one side where the Neumann boundary condition is imposed [14]. In this model POCs are the same as for integrable rectangular billiards and are specified by two coprime integers M, N.

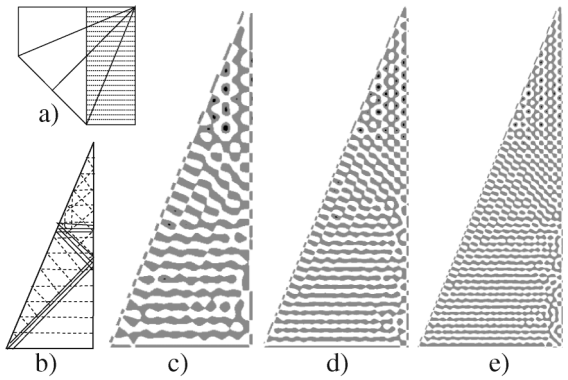

FIG. 1. (a) Unfolded scar state for the simplest POC of the right triangle with angle $\pi/8$. (b) Schematic folding of this state. Dashed lines indicate its maxima. Three solid lines show a region near SD where the unfolded scar function tends to zero. (c)–(e) Eigenfunctions with energy E close to the scar energy $E_{m,n}$. (c) $E = 407.4$; $E_{50,1} = 407.6$. (d) $E = 1015.97$; $E_{79,1} = 1016.12$. (e) $E = 1968.97$; $E_{110,1} = 1969.15$.

The POC length is $l = \sqrt{(2aM)^2 + (2bN)^2}$, where a, b are sides of the rectangle. The usual POCs for rectangular billiard are split (and restricted) by images of the singular point. For odd M each POC is divided into two POCs of width $w = 2ab/l$. Both channels can support scar states, but one requires odd m and the other, even m. When M is even, POC remains unramified and has the width $w = 4ab/l$.

In Figs. 2 and 3 a few examples of high-excited scar states for BB with $(b/a)^2 = \sqrt{5} + 1$ and $ab = 4\pi$ are presented. Black and white regions in these figures correspond, respectively, to positive and negative values of eigenfunctions which are small in regions with irregular nodal patterns. This nodal domain representation is quite sensitive because even a weak noise changes drastically regular nodal pictures. Nevertheless, these (and many other) pictures show high-quality scar structures for BB. Fixing a POC and increasing the energy we always find a reasonably good picture of the corresponding scar state close to the scar energy (3). With increasing energy the perturbation parameter (1) for a given scar decreases, but the number of open scar channels increases [see (7)] and a typical eigenfunction may have contributions from many different scars. Their quantitative description is achieved by computing the overlap of folded scar states $\Psi^{(\mathrm{scar})}_{m,n}(x, y)$ with exact eigenfunctions $\Psi_{E_\lambda}(x, y)$

$$C_{m,n}(E_\lambda) = \int \Psi^{(\mathrm{scar})}_{m,n}(x, y)\Psi_{E_\lambda}(x, y)dxdy. \qquad (9)$$

In computations we fix n and choose m from the condition of minimum of $|E_\lambda - E_{m,n}|$ (when m is kept fixed only one peak appears). In Fig. 4(a) we plot $|C_{m,n}(E)|^2$ versus E with $2000 < E_\lambda < 4000$ for the 1:1 scar state.

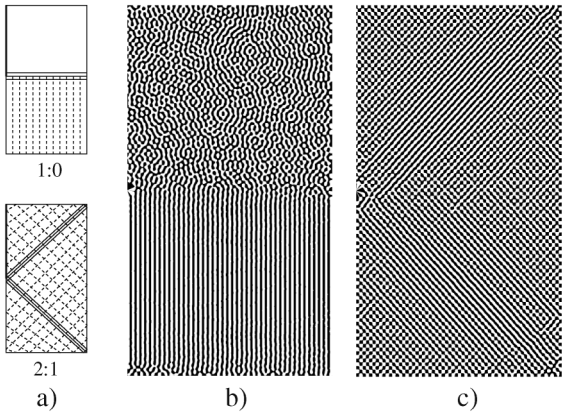

FIG. 2. BB eigenfunctions strongly influenced by 1:0 and 2:1 scar states. (a) Folded scar states for the 1:0 (top) and 2:1 (bottom) periodic trajectories. The thick line shows the part of BB with the Neumann boundary condition. Dashed lines indicate maxima of the scar state. Three solid lines show regions around SD where unfolded scar states tend to zero. (b) Eigenfunction with $E = 10\,209.55$. The 1:0 scar energy $E_{85,1} = 10\,209.65$. (c) Eigenfunction with $E = 10\,017.57$. The 2:1 scar energy $E_{453,1} = 10\,017.67$.

Spikes in such figures confirm that practically near all scar energies (3) there exists true eigenfunctions which have a strong contribution from the given scar state. The analysis of these spikes reveals that their local density

$$\rho_n(E) = \left\langle \sum_\lambda |C_{m,n}(E_\lambda)|^2 \delta(E - E_\lambda + E_{m,n}) \right\rangle_m \qquad (10)$$

averaged over different m can well be approximated by the Breit-Wigner distribution [see Fig. 4(b)]

$$\rho_n(E) = \frac{\Gamma_n(E)}{2\pi\{[E - \epsilon_n(E)]^2 + \Gamma_n^2(E)/4\}} \qquad (11)$$

similar to the one observed in random band matrices with preferential basis [15]. For the 1:1 scar state the best fit gives $\Gamma_n \approx 3.5n^2/\sqrt{k}$ which agrees qualitatively with an estimate which can be obtained from [11] that for BB the total width of a given scar state in the leading order is $\Gamma_n(E) \sim (n^2/w^2)\sqrt{l/kw^2}$.

For Veech billiards the density of scar states is of the same order as the total density of states [cf. (8)] and one is led to the conjecture that their eigenfunctions can be represented as a sum over scar states,

$$\Psi_{E_\lambda}(x, y) = \sum_{\mathrm{scars}} C_{m,n}(E_\lambda)\Psi^{(\mathrm{scars})}_{m,n}(x, y). \qquad (12)$$

An important characteristic of wave functions is a set of participation ratios (see, e.g., [16,17] and references therein)

$$R_q(E) = \left(\sum_{m,n} |A_{m,n}(E)|^{2q} \right)^{-1}, \qquad (13)$$

where $A_{m,n}(E)$ are coefficients of the expansion of wave functions in a suitable basis normalized such that $\sum_{m,n}|A_{m,n}|^2 = 1$. PI systems, as all systems with intermediate statistics, should have some fractal properties

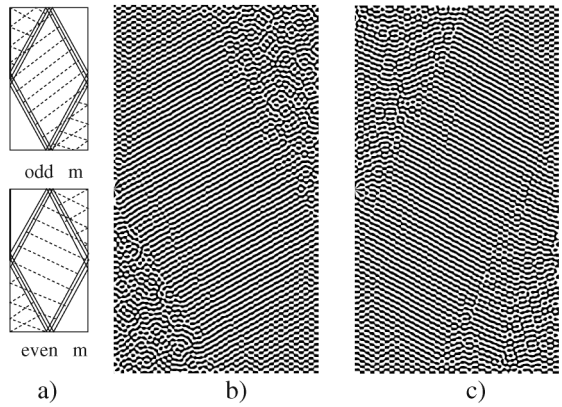

FIG. 3. The same as in Fig. 2 but for 1:1 scar states. (a) Folded scar states for 1:1 POCs with even and odd m. (b) Eigenfunction with $E = 10\,041.41$. The 1:1 scar energy $E_{347,1} = 10\,041.87$. (c) Eigenfunction with $E = 10\,099.58$. The 1:1 scar energy $E_{348,1} = 10\,099.82$.

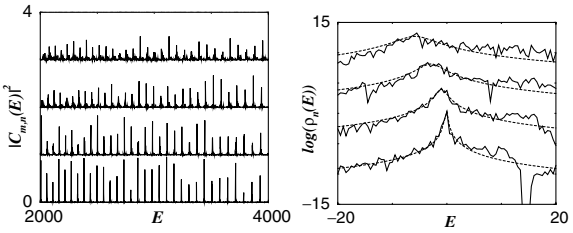

a) b)

FIG. 4. (a) Overlap of exact eigenfunctions of BB with the 1:1 scar state with (from bottom to top) $n = 1, 2, 3, 4$ (graphs for different n are shifted up for clarity by $n - 1$ units). (b) Local density (10) for this overlap [graphs with different n are shifted up by $5(n - 1)$ units]. Dashed lines indicate the best fit in the Breit-Wigner form (11).

[16] and it is natural to expect that $R_q(E) \overset{k\to\infty}{\to} k^{D_q(q-1)}$ with fixed D_q called generalized fractal dimensions (see, e.g., [16,17]).

Under the simplest assumption that for scar states the local density of $|C_{m,n}(E)|^{2q}$ is proportional to $\rho_n^q(E)$ with the Breit-Wigner form (11) of $\rho_n(E)$, (12) and (11) with the above estimate for Γ_n give $D_q = 0.5$ confirming the fractal character of BB eigenfunctions in momentum representation. In Fig. 5 we plot R_q for $q = 2$ and $q = 3$ for BB computed directly from the expansion of eigenfunctions into trigonometric series. The best fits $R_2 \approx 2.52\sqrt{k}$ and $R_3 \approx 4.7k$ very well describe the data in the given interval of energy which means that for BB $D_2 \approx D_3 \approx 0.5$ in accordance with the above estimates. The assumed value of spectral compressibility for BB, $\chi = 0.5$ [14], is close to the spectral compressibility $\chi(D_2)$ numerically computed at the point $D_2 = 0.5$ for the critical power-law random band matrix model (cf. Fig. 2 of [17]).

In summary, we have argued that strong diffraction in PI systems leads to the formation of a new type of long-lived resonant states (scar states) propagating inside POC and reflecting from SD as from perfect mirrors. Many true eigenfunctions of such models have surprisingly clear structures associated with such states even at high energies. It follows from our results that PI models are the best models of scar phenomenon. For good PI models (Veech billiards) the density of scar states is a constant, and they can be considered as the basis of perturbation expansion. A weak residual interaction between them (neglected in this Letter) forms true eigenstates and leads to an intermediate character of spectral statistics for these models. It appears that this interaction shares many features with the critical random band matrix model. We have also checked that BB wave functions have fractal properties in momentum space. Though we have discussed only PI models a certain form of superscarring

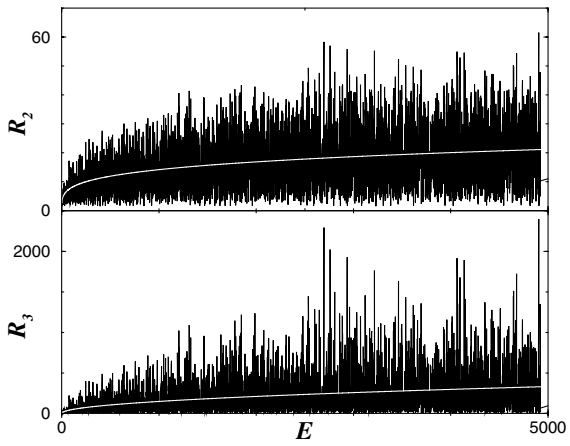

FIG. 5. Participation ratios R_2 (top) and R_3 (bottom) versus energy for BB. White lines indicate the fits $R_2 \approx 2.52\sqrt{k}$ and $R_3 \approx 4.7k$.

seems to exist also in general plane polygonal billiards because of two main ingredients of the discussed mechanism: strong diffraction and the existence of POCs are both presented in such systems.

*Unité de recherche de l'Université de Paris XI associée au CNRS.

[1] O. Bohigas, M.-J. Giannoni, and C. Schmit, Phys. Rev. Lett. **52**, 1 (1984).
[2] M.V. Berry, J. Phys. A **10**, 2083 (1977).
[3] P.J. Richens and M.V. Berry, Physica (Amsterdam) **2D**, 495 (1981).
[4] E.B. Bogomolny, U. Gerland, and C. Schmit, Phys. Rev. E **59**, R1315 (1999).
[5] B.I. Shklovskii *et al.*, Phys. Rev. B **47**, 11487 (1993).
[6] E.J. Heller, Phys. Rev. Lett. **53**, 1515 (1984).
[7] L. Kaplan and R.J. Heller, Ann. Phys. (N.Y.) **264**, 171 (1998).
[8] A. Sommerfeld, *Optics* (Academic, New York, 1954).
[9] E. Bogomolny, O. Giraud, and C. Schmit, Commun. Math. Phys. **222**, 327 (2001).
[10] J.F. Carlson and A.E. Heins, Q. Appl. Math. **4**, 313 (1947).
[11] E. Bogomolny and C. Schmit, Nonlinearity **16**, 2035 (2003).
[12] B.W. Batterman and H. Cole, Rev. Mod. Phys. **36**, 681 (1964).
[13] W.A. Veech, Invent. Math. **97**, 533 (1989).
[14] J. Wiersig, Phys. Rev. E **65**, 046217 (2002).
[15] Ph. Jacquod and D.L. Shepelyansky, Phys. Rev. Lett. **75**, 3501 (1995).
[16] J.T. Chalker, V.E. Kravtsov, and I.V. Lerner, JETP Lett. **64**, 386 (1996).
[17] F. Evers and A.D. Mirlin, Phys. Rev. Lett. **84**, 3690 (2000).